A THEMIS survey of flux ropes and traveling compression regions: Location of the near-Earth reconnection site during solar minimum

S. M. Imber,[1] J. A. Slavin,[1] H. U. Auster,[2] and V. Angelopoulos[3]

Received 16 August 2010; revised 27 September 2010; accepted 20 October 2010; published 1 February 2011.

[1] A statistical study of flux ropes and traveling compression regions (TCRs) during the Time History of Events and Macroscale Interactions during Substorms second tail season has been performed. A combined total of 135 flux ropes and TCRs in the range GSM X ~ −14 to −31 R_E were identified, many of these occurring in series of two or more events separated by a few tens of seconds. Those occurring within 10 min of each other were combined into aggregated reconnection events. For the purposes of this survey, these are most likely the products of reconnection occurring simultaneously at multiple, closely spaced x-lines as opposed to statistically independent episodes of reconnection. The 135 flux ropes and TCRs were grouped into 87 reconnection events; of these, 28 were moving tailward and 59 were moving Earthward. The average location of the near-Earth x-line determined from statistical analysis of these reconnection events is (X_{GSM}, Y^*_{GSM}) = (−30R_E, 5R_E), where Y* includes a correction for the solar aberration angle. A strong east-west asymmetry is present in the tailward events, with >80% being observed at GSM Y* > 0. Our results indicate that the Earthward flows are similarly asymmetric in the midtail region, becoming more symmetric inside −18 R_E. Superposed epoch analyses indicate that the occurrence of reconnection closer to the Earth, i.e., X > −20 R_E, is associated with elevated solar wind velocity and enhanced negative interplanetary magnetic field B_Z. Reconnection events taking place closer to the Earth are also far more effective in producing geomagnetic activity, judged by the *AL* index, than reconnection initiated beyond X ~ −25 R_E.

Citation: Imber, S. M., J. A. Slavin, H. U. Auster, and V. Angelopoulos (2011), A THEMIS survey of flux ropes and traveling compression regions: Location of the near-Earth reconnection site during solar minimum, *J. Geophys. Res.*, *116*, A02201, doi:10.1029/2010JA016026.

1. Introduction

[2] As described by the near-Earth neutral line model of substorms [*Hones*, 1977; *Baker et al.*, 1996], the erosion of magnetic flux at the dayside magnetopause results in an increase in tail lobe flux and a thinning of the cross-tail current sheet leading to reconnection at one or more locations. Initially, reconnection involves only highly stretched, closed field lines and proceeds slowly. Flux ropes (FRs) are formed between the reconnection sites, as shown in Figure 1 [*Hesse et al.*, 1996; *Shay et al.*, 2003]. The nonzero B_Y in the plasma sheet causes these structures to have helical topologies with a core field oriented largely in the dawn-dusk direction. Ion tearing-based models of multiple x-line reconnection have one x-line outpacing the others and eventually reconnecting lobe field lines. The high Alfven speed in the lobes causes the reconnection rate at this x-line (now called the dominant x-line) to increase significantly, resulting in x-lines and flux ropes on either side of this site being swept away from it, toward the Earth, or down the tail [*Schindler*, 1974; *Slavin et al.*, 2003, 2005; *Sitnov et al.*, 2009].

[3] Traveling compression regions (TCRs) are compressions in the lobe magnetic field that have been observed to travel both Earthward and tailward at speeds of a few hundred kilometers per second. *Slavin et al.* [1984] proposed that these are caused by flux ropes which locally enhance the plasma sheet thickness, compressing the lobe field (Figure 1). Flux ropes and TCRs have been studied extensively in the near tail using spacecraft such as Geotail and Cluster [e.g., *Slavin et al.*, 1998, 2005; *Eastwood et al.*, 2005], in the midtail using IMP-8 [e.g., *Taguchi et al.*, 1998], and in the distant tail using ISEE-3 and Geotail [e.g., *Sibeck et al.*, 1984; *Slavin et al.*, 1993; *Kawano et al.*, 1994].

[4] Dawn-dusk asymmetries in the observations of a variety of reconnection-related signatures have been reported previously. *Nakamura et al.* [1991] showed an asymmetric distribution of high-speed plasma sheet flows in Active Magnetospheric Particle Tracer Explorers Ion Release

[1]NASA Goddard Space Flight Center, Greenbelt, Maryland, USA.
[2]Institut für Geophysik und Extraterrestrische Physik, Technische Universität Braunschweig, Braunschweig, Germany.
[3]Institute of Geophysics and Planetary Physics, University of California, Los Angeles, California, USA.

0148-0227/11/2010JA016026

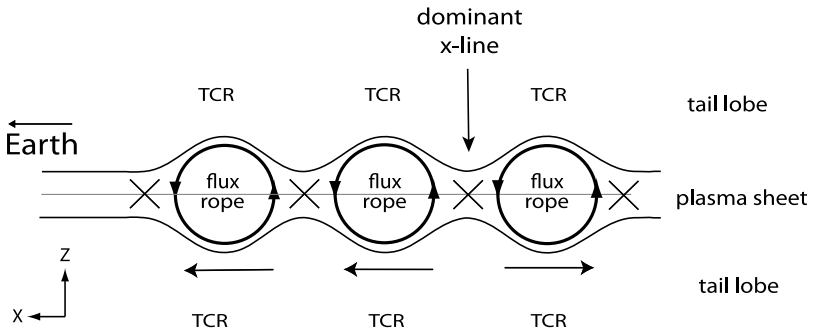

Figure 1. A schematic to show the formation of multiple x-lines in the magnetotail in the GSM X-Z plane.

Module data between 10 and 19 R_E downtail and attributed it to the orbit of the observing spacecraft. *Angelopoulos et al.* [1994] observed a small bias toward dusk when observing Earthward and tailward high-speed plasma sheet flows in ISEE 2 data and put forward the explanation that diamagnetic drifts caused by Earthward particle pressure gradients skew the observations. More recently, *Slavin et al.* [2005] performed a statistical study of Cluster magnetic field data and observed significantly more TCRs on the dusk side of the tail than on the dawn side in the region $X > -20$ R_E. *Raj et al.* [2002] used Wind data to show an asymmetric distribution of Earthward bulk flows that were displaced toward dusk. Of 51 flows identified, 50 were within $X > -15$ R_E, and 41 were displaced toward dusk. *Nagai and Machida* [1998] have shown an asymmetric distribution of both tailward- and Earthward-moving flow bursts observed by Geotail in the region −10 to −50 R_E. *Nagai et al.* [1998] showed that tailward fast flows related to substorm onsets were most frequently observed on the dusk side, although they also observed that Earthward flows in the region $-30 < X < -5$ R_E appear to be symmetric. A summary of these results is presented in Table 1.

[5] The Time History of Events and Macroscale Interactions during Substorms (THEMIS) mission consists of five spacecraft launched in February 2007 into equatorial orbits [*Sibeck and Angelopoulos*, 2008]. The outer pair of spacecraft had apogees at −20 and −31 R_E during this period that corresponded to an orbital period of 2 and 4 days, respectively. One advantageous feature of the equatorial orbit of the THEMIS spacecraft is that they spend an equal amount of time in the dawn and dusk sectors per orbit, therefore any asymmetry is unlikely to be due to orbital bias.

[6] In this study, we identify flux ropes and TCRs in the outer pair of THEMIS spacecraft and thereby determine the statistical location of the reconnection site in the tail. These measurements are of particular interest because they occur during the quietest solar minimum of recent decades, with a 50 year low in solar wind pressure and no sunspots observed on 78 of the first 90 days of 2009. This resulted in extremely low solar wind velocities and interplanetary magnetic field strengths. These rare conditions provide an opportunity to study tail dynamics under low dayside driving conditions.

2. General Features of Flux Ropes, Dipolarization Fronts, and Traveling Compression Regions

[7] Three types of magnetic structures generated by reconnection in the magnetotail are outlined in this section: dipolarization fronts (DFs), flux ropes, and traveling compression regions. Figure 2 shows an example of each structure taken from the literature, Figure 2a is a dipolarization observed by THEMIS D [from *Runov et al.*, 2009], Figure 2b is a flux rope observed by Geotail [from *Slavin et al.*, 2003], and Figure 2c is a TCR observed by Cluster [from *Slavin et al.*, 2005]. Figures 2a–2c show the GSM X, Y and Z components of the magnetic field and the total field at the bottom. The vertical and horizontal scales are identical in each panel.

[8] DFs in the tail are generated by the pileup of field lines in the near-Earth region ahead of reconnection-driven bursty bulk flows (BBFs) [e.g., *Hesse et al.*, 1996]. The total signature is only a few seconds long and is characterized by a large increase in the B_Z component of the magnetic field. In some cases, DFs may be preceded by a small negative B_Z. This negative B_Z has been attributed to a sudden late growth phase increase in the cross-tail current intensity [*Ohtani et al.*, 1992].

[9] Flux ropes are helical magnetic structures formed between pairs of x-lines. They are characterized by a bipolar B_Z signature, coincident with a peak in the B_Y component corresponding to the strong core field (Figure 2b). The total

Table 1. A Summary of Observations of the East-West Location of Reconnection-Related Flows and Structures in the Tail

Author	Spacecraft	Tail Region (R_E)	Reconnection Phenomena	Earthward Flow	Tailward Flow
Nagai et al. [1998]	Geotail	10–30	Flow bursts	Symmetric	Skewed to dusk
Nagai and Machida [1998]	Geotail	10–20	Convection flows	Skewed to dusk	Skewed to dusk
Nakamura et al. [1991]	AMPTE IRM[a]	10–19	Plasma sheet flows	Skewed to dusk	N/A
Slavin et al. [2005]	Cluster	11–19	FR/TCRs[a]	Skewed to dusk	Skewed to dusk
Angelopoulos et al. [1994]	ISEE 2	Inside 22 R_E	Plasma sheet flows	Small skew to dusk	Small skew to dusk
Raj et al. [2002]	Wind	Mostly inside 15 R_E	Convective flows	Skewed to dusk	N/A

[a]AMPTE IRM, Active Magnetospheric Particle Tracer Explorers Ion Release Module; FR, flux rope; TCRs, traveling compression regions.

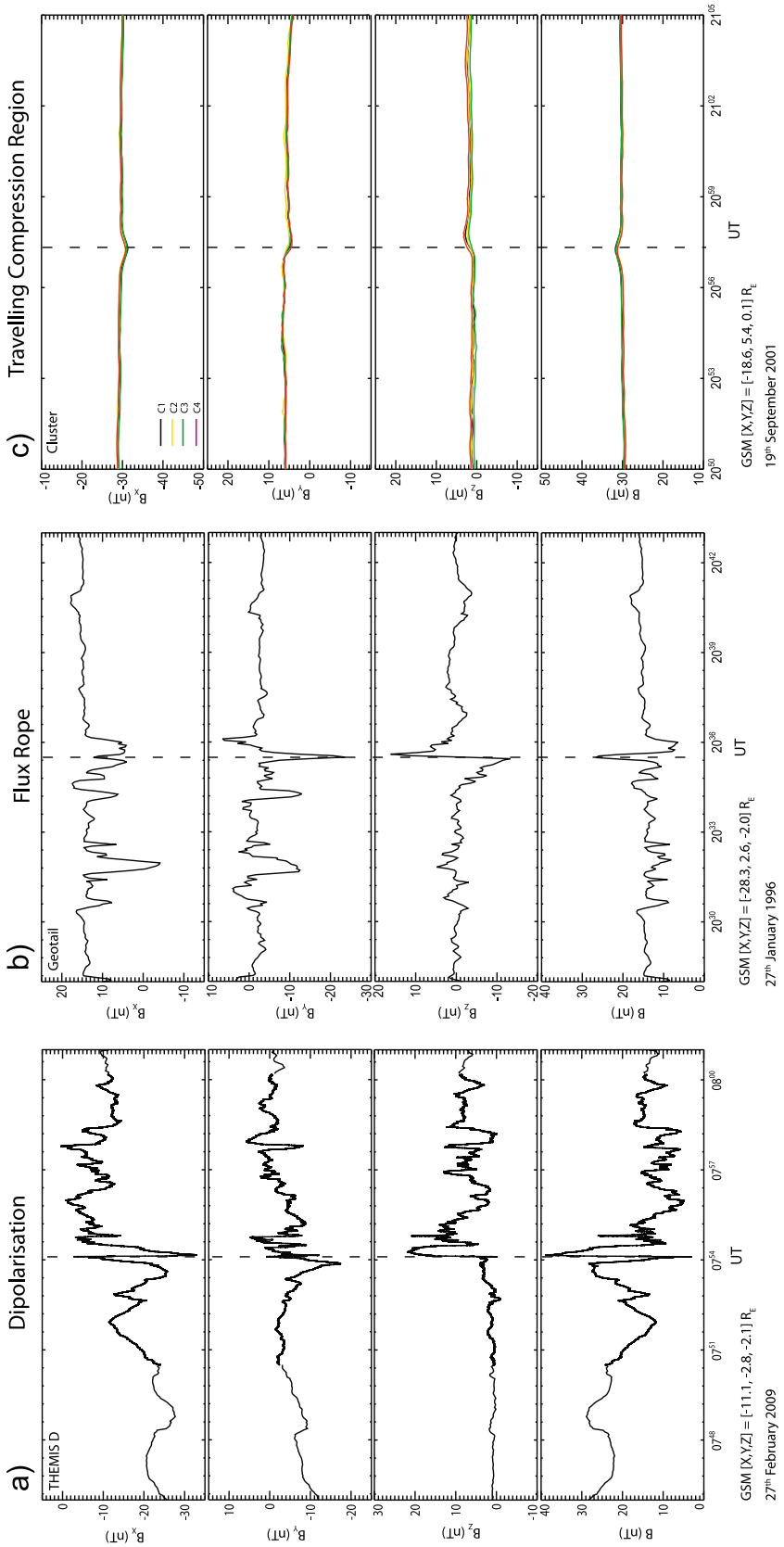

Figure 2. Examples of (a) a dipolarization signature observed by THEMIS D [from *Runov et al.*, 2009], (b) a flux rope at Geotail [from *Slavin et al.*, 2003], and (c) a TCR at Cluster [from *Slavin et al.*, 2005]. The horizontal and vertical scales are the same for each panel.

field strength therefore also maximizes at the center of the bipolar signature. In situ observations of flux ropes have been made as close as 14 R_E [e.g., *Slavin et al.*, 2003] and as far downtail as 220 R_E [e.g., *Hones et al.*, 1984; *Moldwin and Hughes*, 1992]; however, they are most frequently formed in the near-tail region (20–30 R_E downtail) in agreement with the near-Earth neutral line model [e.g., *Nagai et al.*, 1998]. The duration of a flux rope is measured from the minimum to the maximum of the bipolar B_Z signature and typically ranges from ~30 s in the near tail to ~1–2 min in the distant tail [*Ieda et al.*, 1998; *Slavin et al.*, 2003]. Flux ropes can be observed moving Earthward or tailward and are generally embedded in a region of high speed flow and high plasma beta.

[10] DFs observed in spacecraft data are distinguished from Earthward-moving flux ropes by (1) their short duration: ~1 s rise time [e.g., *Sergeev et al.*, 2009; *Runov et al.*, 2009] as opposed to ~10 s of seconds for flux ropes, (2) their lack of a well-defined $\pm B_Z$ followed by continued positive B_Z attributed to lobe reconnection, and (3) their lack of a strong B_Y "core" field centered on the $\pm B_Z$ signature. In addition, Earthward propagating flux ropes are generally observed in the plasma sheet tailward of $X \sim -14$ R_E [*Slavin et al.*, 2003], whereas dipolarization fronts are have their greatest amplitude and are most frequently observed near the flow braking region, ~−10 R_E [e.g., *Saito et al.*, 2010].

[11] TCRs are observed by spacecraft located in the lobes of the tail and are generated by the motion of a flux rope traveling in the plasma sheet beneath the spacecraft. The compression of the lobe field lines generates a peak in both the B_X component of the magnetic field and the total field strength as well as a bipolar signature in the B_Z component. If sufficient plasma is present in the lobes, a $\pm V_Z$ signature may be observed as the flux tubes are displaced upward and downward by the passage of the underlying flux rope [e.g., *Kawano et al.*, 1994]. The typical example displayed in Figure 2c shows that the TCR signature is generally much smaller in magnitude and slightly longer in duration than the flux rope signature.

3. THEMIS Observations of FRs and TCRs

[12] The orbits of the THEMIS spacecraft were adjusted prior to the second tail season such that both spacecraft spent more time in or near the neutral sheet. We have therefore focused our statistical study on this second tail season and identified both flux ropes and TCRs in the THEMIS B and C magnetic field and plasma data during the time period December 2008 to April 2009. Conjunctions between this outermost pair of spacecraft were identified when both were within 20 R_E in GSM Y from the center of the tail. In addition, B and C were required to be at least 20 and 14 R_E downtail, respectively.

[13] Magnetic field data at 3 s (spin) resolution in 10 min duration segments [*Auster et al.*, 2008] were visually inspected to identify flux ropes and TCRs. The magnetic signature used to identify a flux rope in this study is a bipolar variation in the B_Z component passing through $B_Z = 0$, at the center of which is an enhancement in the B_Y component corresponding to the strong core field of the flux rope. This core field is also seen as a peak in the total field, B. These signatures are often accompanied by fast plasma sheet flows and a corresponding high plasma beta. These plasma signatures were not required, however, because they are very sensitive to how deeply the spacecraft penetrate into the flux rope. These selection criteria are similar to previous statistical flux rope studies such as those by *Moldwin and Hughes* [1992], *Ieda et al.* [1998], *Slavin et al.* [2003], and *Henderson et al.* [2006]. Most recently, criteria similar to these have been used to identify plasmoids at Mercury [*Slavin et al.*, 2009], Jupiter [*Kronberg et al.*, 2007; *Vogt et al.*, 2010], and Saturn [*Hill et al.*, 2008; *Jackman et al.*, 2007].

[14] A TCR is defined in this study by a bipolar ΔB_Z signature relative to the background field, which is generally biased positive or negative because of tail flaring. The B_Z signature is therefore frequently displaced from $B_Z = 0$, and the signature used is $\pm\Delta B_Z$ [see *Taguchi et al.*, 1996]. The compression of the lobes by the underlying flux rope is characterized by an enhancement in the B_X component and a peak in the total field, B. No corresponding V_X or plasma beta enhancement is expected unless the spacecraft encounter skims the outer layers of the flux rope and the surrounding plasma sheet boundary layer [e.g., *Slavin et al.*, 2005]. All TCRs in this study had a compression ratio $\left(\Delta B/B\right)$ of >1%, and the selection criteria outlined above are in agreement with previous studies by *Taguchi et al.* [1996] and *Slavin et al.* [2005].

[15] The 3 s resolution of the data and the visual inspection of 10 min intervals impose limits on the duration of events selected. The duration of a flux rope or TCR is defined as the time between the minimum and maximum of the B_Z signature. The shortest event accepted in this study has a duration set by the Nyquist condition of 6 s, while events up to 5 min in duration would also be readily identified. In practice, all events fall between 6 and 110 s.

[16] An example of a flux rope observed by the fluxgate magnetometer on THEMIS C is in Figure 3(left). During this time period, the instrument was in burst mode, taking measurements at 128 vectors/s. A clear bipolar signature passing through $B_Z = 0$ is evident in Figure 3c, coincident with an enhancement in the B_Y component and the total field (Figures 3b and 3d) marked by a vertical dashed line. The sense of the B_Z variation, south then north (SN), indicates that it is traveling Earthward, and the duration is 6.2 s. The plasma beta is ~0.2, and the spacecraft is observing fast Earthward flow (~400 km/s) as measured by the electrostatic analyzer instrument [*McFadden et al.*, 2008]. An example of a TCR signature observed by THEMIS B is displayed in Figure 3(right), which is a 4 min interval of magnetic field data. A bipolar B_Z signature is observed, first north then south (NS) with a peak-to-peak duration of 45 s. This is coincident with a peak in B_X signifying lobe compression. The plasma data are not displayed as the spacecraft is deep in the lobes and the plasma is too tenuous to be measured.

[17] Based on the selection criteria outlined above, 135 flux ropes and TCRs were identified in the data. If two signatures were identified within 10 min of each other, then these were classified as a single reconnection interval as they are likely to have been formed near-simultaneously because of reconnection at multiple x-lines. We chose 10 min because this was identified by *Angelopoulos et al.* [1994] and *Nagai et al.* [1998] as the characteristic time scale for reconnection

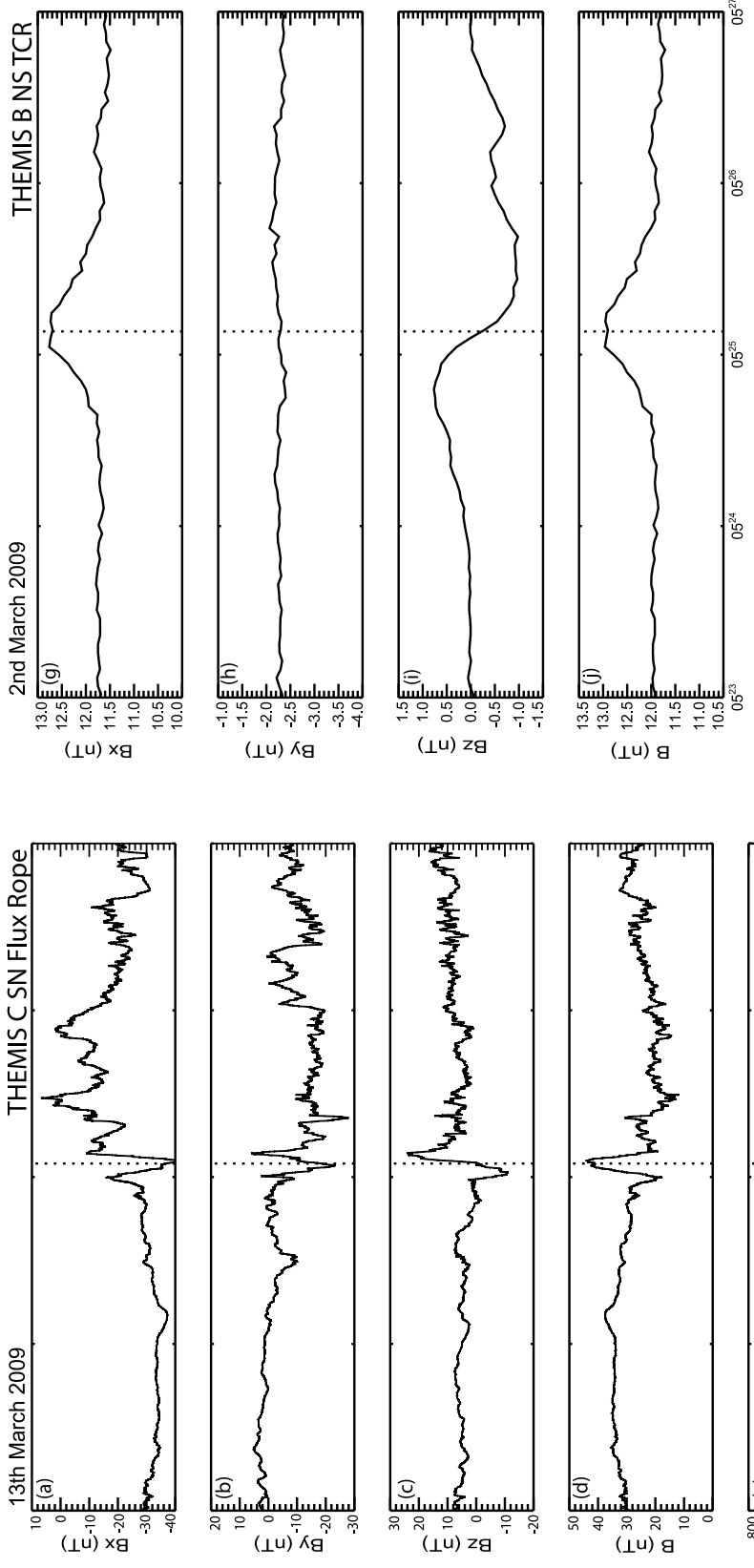

Figure 3. (a–f) An SN flux rope observed by THEMIS C on 13 March 2009. Figures 3a–3d are the GSM components of the magnetic field, Figure 3e is the velocity in the GSM X direction measured by the spacecraft, and Figure 3f is the plasma beta. (g-j) An NS TCR observed by THEMIS B on 2 March 2009. A vertical dashed line in each figure marks the center of the signature.

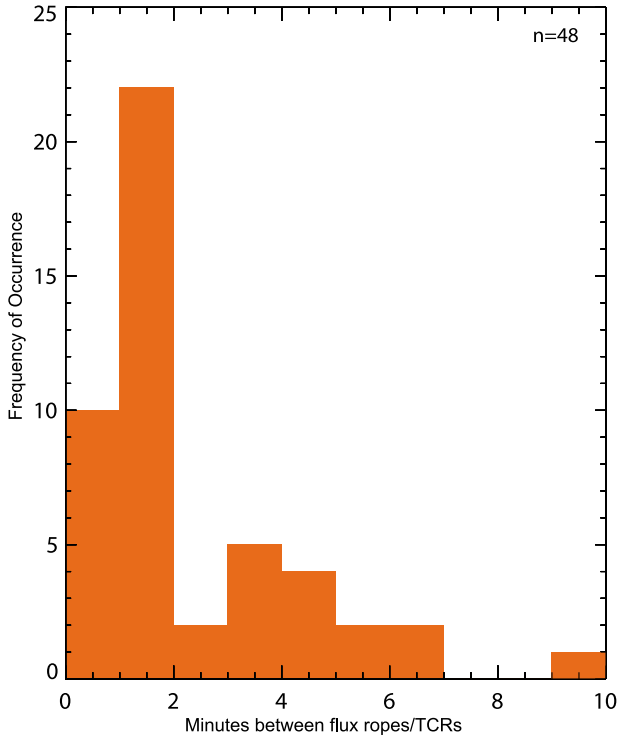

Figure 4. The occurrence distribution of the number of minutes between flux ropes or TCRs grouped together into single reconnection intervals.

in the tail. By these criteria, the 135 FR/TCRs correspond to a total of 87 individual reconnection events. The occurrence distribution of the time between flux ropes within a group is displayed in Figure 4. Of the 48 flux ropes/TCRs that were grouped together, 32 were observed within 2 min of another event, and an additional 11 were observed within 5 min. The average separation of successive FR/TCRs in a group is 2.5 min, and only on five occasions is the separation greater than 5 min. We have investigated changing the threshold time between events and find that even if we shortened this time to 5 min [after *Nakamura et al.*, 2001] or extended the time to over 15 min [after *Slavin et al.*, 1993, 2005] we get very similar results.

[18] Twenty-eight of the 87 reconnection events were observed traveling tailward (an NS signature), and 59 were traveling Earthward (SN). Previous studies of flux ropes and TCRs with Geotail [e.g., *Slavin et al.*, 2003] have produced roughly equal numbers of SN and NS events in the region X ~ −14 to −31 R_E. This bias toward Earthward propagation can be easily understood when the THEMIS orbits are considered. The inner spacecraft that would be expected to predominantly observe Earthward-moving events has a 2 day orbit, while the most distant spacecraft has a 4 day orbit and would be expected to observe predominantly tailward-moving (NS) flux ropes and TCRs. Figure 5a shows the number of hours the spacecraft spent at each GSM X location. A larger number of SN signatures is expected in this study given the number of hours spent within −20 R_E, and the ratio of the SN to NS signatures is therefore in approximate agreement with previous studies. It must be stressed, however, that the location of the reconnection site is not expected to be steady for any significant amount of time despite the low solar activity during this period. This is reflected in the fact that both spacecraft frequently observed both SN and NS flux ropes, as described in more detail below.

4. Analysis

4.1. The Average Location of the Near Earth Neutral Line

[19] Previous studies have used a variety of methods to determine the location of the reconnection site, such as observations of highly energetic electrons [*Nagai et al.*, 2005] and high-speed plasma flow [e.g., *Hones and Schindler*, 1979; *Nishida et al.*, 1981; *Angelopoulos et al.*, 1994]. Most of these previous studies have placed it in the range −15 to −30 R_E [see review by *Nagai*, 2006]. Assuming that, on average, the x-line is somewhere in this range, it would be expected that the majority of observations within ~20 R_E would be of the SN type (Earthward moving). The ratio of

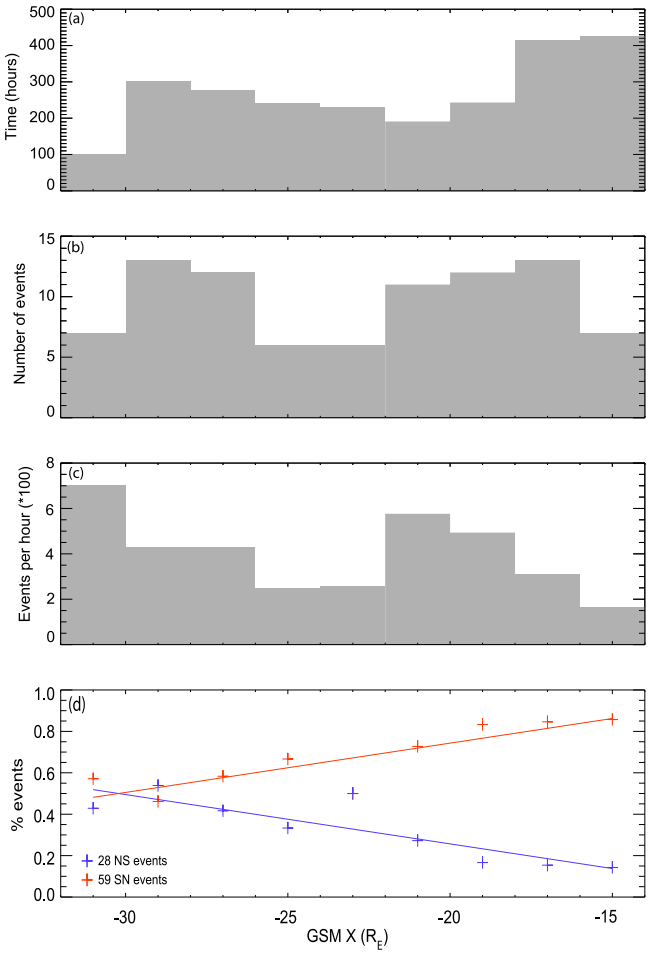

Figure 5. (a) A histogram of the number of hours that THEMIS B and C spent between GSM X = −14 and −31 R_E. (b) The number of reconnection events observed in each GSM bin of width 2 R_E. (c) The number of events observed per hour of observation time (*100). (d) The percentage of events in each bin that are NS (blue) and SN (red). The lines are linear fits to the data points.

SN-to-NS observations will decrease with increasing distance from the Earth such that eventually equal numbers are observed at the average location of the reconnection site. Beyond that location, we would expect to observe more NS flux ropes and TCRs. Figure 5b shows the total number of reconnection events observed in each GSM X bin of 2 R_E width. The number of events per hour of observation time is shown in Figure 5c (multiplied by a factor of 100), showing a falloff in the number of events within −18 R_E. This is expected as the x-line rarely forms within this location, and therefore NS FR/TCRs are not frequently observed this close to the Earth. In addition, Earthward-moving FRs will reconnect with the Earth's dipolar field, which may also reduce the total number of FRs/TCRs observed closest to the Earth. Beyond −26 R_E, the number of events per hour fluctuates about a mean value of approximately 0.04 per hour.

[20] Figure 5d displays the percentage of NS and SN flux ropes/TCRs in each 2 R_E bin such that each individual bin sums to 1. Linear fits to the data have been plotted in red for the SN and blue for the NS events. It is clear from Figure 5d that, as expected, in the near-Earth region nearly all of the observations are of Earthward (SN) FR/TCRs. The ratio of SN-to-NS observations becomes equal somewhere in the region of −30 R_E, and we therefore estimate that the average location of the near-Earth reconnection site is at this location. If we assume that the distribution of locations is approximately Gaussian about a mean position, then this average location, −30 R_E, is also the most probable location of the reconnection site. If the distribution is skewed or multipeaked, however, then the average location may not be the most probable. The linear fits to the data appear to be very good, therefore we have some confidence in this result. Unlike previous studies, which have either placed the reconnection site within a large range in the X direction or have only estimated its occurrence frequency beyond the spacecraft apogee, Figure 5d can be used to estimate the likelihood of reconnection taking place Earthward or tailward of any location in the range −14 to −31 R_E.

[21] *Nagai et al.* [2005] placed the average location of the reconnection site between −20 and −30 R_E, while *Slavin et al.* [2005] placed the reconnection site tailward of the Cluster apogee (−19 R_E) 80% of the time. The extremely quiet solar activity during THEMIS tail campaigns is the most likely reason for the reconnection site being located further downtail than during more active times. This is discussed in further detail below.

4.2. The Influence of Upstream Conditions

[22] The solar wind conditions have been shown to modulate the low-latitude dayside reconnection rate [e.g., *Kan and Lee*, 1979], and this in turn determines the amount of open flux (and the stress level) in the tail. Ultimately, this would be expected to influence the location of the near-Earth reconnection site. *Slavin et al.* [2005] surveyed TCRs using Cluster data and found that the average intensity of the lobe field during tailward-moving TCR observations at X > −19 R_E was ~32 nT while for Earthward TCRs it was ~27 nT. *Nagai et al.* [2005] demonstrated a weak dependence of the location of the x-line on solar wind electric field, $V_X B_Z$, and no dependence on solar wind pressure. They also found a higher average solar wind speed for the near-tail (X > −25 R_E) compared to the more distant x-lines (−25 > X > −31 R_E). In our study, the exact location of the x-line is not known; however, it is possible to bin together all observations of NS (tailward-moving) flux ropes and TCRs within X = −20 R_E and determine the average solar wind conditions that led to the initiation of reconnection within this region. These results can then be compared with the average solar wind conditions leading to reconnection tailward of −25 R_E by considering all Earthward-moving flux ropes and TCRs that were observed beyond that distance.

[23] Figure 6a presents a superposed epoch analysis of the solar wind speed for each of these cases, along with the interplanetary magnetic field (IMF) B_Z component and the solar wind pressure for 1 hour before and 30 min after t_0 (the time of the event observation). It is possible that reconnection was initiated several minutes prior to the observation of the flux rope or TCR in some cases, so t_0 is not the exact time of reconnection onset. The dotted line is upstream data corresponding to cases in which reconnection was known to have been initiated within −20 R_E (5 NS events identified within −20 R_E), whereas the solid line is for events in which reconnection took place beyond −25 R_E (19 SN events beyond −25 R_E). The near-Earth reconnection events appear to be related to solar wind speeds ~30–50 km/s higher than the midtail events. The near-Earth events also appear to be associated with periods of more strongly southward IMF orientation, particularly between t = −45 and −15 min. Combining these results, this is an indication that prior to reconnection onset in the near-Earth region, the solar wind driving (given by VB_Z for southward IMF) is higher than for onset in the midtail region. Finally, there does not appear to be any dependence on the solar wind pressure. Our results show good agreement with *Nagai et al.* [2005], who also suggest that reconnection onsets nearer the Earth are related to periods when the recent solar wind driving conditions on the dayside are higher.

[24] The average location of the dominant x-line during the time period encompassed in this study was found to be further tailward than most previous estimates [see review by *Nagai*, 2006]. One likely explanation for this is that these observations were made during an extended period of reduced solar activity that is correlated with lower solar wind driving. The above result suggests that this will lead to an average reconnection location further downtail than during more active times.

[25] To put these data into context, a superposed epoch analysis of the THEMIS B_Z measurements are presented in Figures 6d and 6e for all 59 SN and 28 NS events. The typical bipolar signature of a flux rope/TCR is clearly evident at t_0 and was a key signature by which the events were selected. The SN signature in Figure 6d does not pass through zero, indicating that a significant portion of the events were TCRs as opposed to flux ropes. The NS signature in Figure 6e does go through zero, however, therefore a higher percentage of the observed events were flux ropes. This could be because the average diameter of the NS flux ropes was larger than that of the SN flux ropes such that a spacecraft near the neutral sheet would be more likely to sample the flux rope rather than the associated lobe compression. The relative orbits of the THEMIS spacecraft may also have caused this difference, particularly if the tailward spacecraft was more frequently located in or near the neutral sheet.

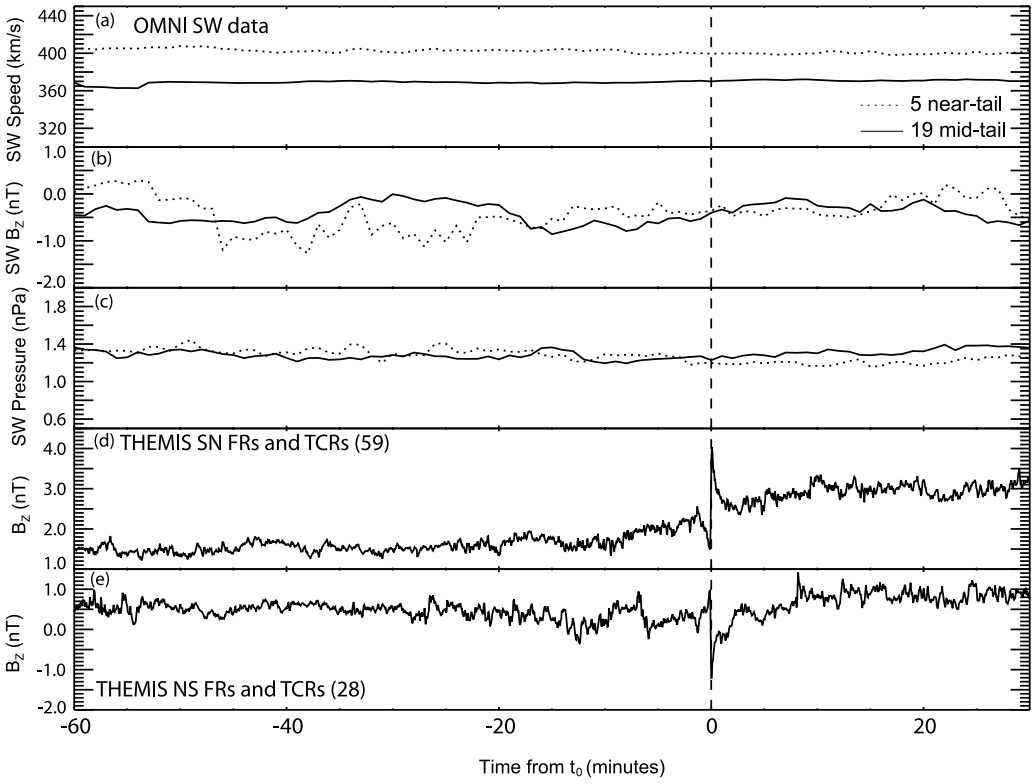

Figure 6. Superposed epoch analyses of the upstream solar wind conditions 60 min before to 30 min after the event identification in the THEMIS spacecraft data (a) solar wind speed, (b) IMF B_Z, and (c) solar wind pressure. The dotted line is the data corresponding to the 5 events when reconnection was known to have been initiated in the near-tail region, whereas the solid line is for the 19 midtail events. (d and e) Superposed epoch analyses of the THEMIS magnetic field B_Z component for all 59 SN and 28 NS events.

4.3. Substorm Association

[26] Flux ropes and TCRs have been shown to be associated with enhanced geomagnetic activity as measured by chains of ground-based magnetometers [e.g., *Slavin et al.*, 2005]. This is to be expected as flux ropes are formed by reconnection, the same process in the near-tail that leads to auroral activity and enhancement of the electrojet currents. Thirty-six of 87 events identified here can be associated with enhanced geomagnetic activity as identified using the *AL* index ($AL < -100$ nT). It should be noted that the *AL* index can miss significant electrojet enhancements because of poor spatial coverage of the auroral region.

[27] Figure 7 shows two additional examples of events included in this study. An NS flux rope observed by THEMIS C is shown in Figures 7b–7f. Velocity data were not available for this interval; however, plasma beta was >1.7, indicating that the spacecraft was located in the outer edge of the plasma sheet, and there is an enhancement in B_Y coincident with the bipolar signature in B_Z. Finally, the B_Z signature passes through zero, which is another criteria for a flux rope. The observing spacecraft was located at -19 R_E, therefore the x-line was formed Earthward of this location. A 4 h interval of *AL* data for 4 March 2009 is plotted in Figure 7 (top), and it is clear that this flux rope was observed during a period of enhanced geomagnetic activity.

[28] Figures 7h–7k show an SN TCR, which formed tailward of the location of THEMIS B, 27 R_E downtail, on 23 February 2009. The corresponding *AL* index for a 4 h period is shown in Figure 7g and demonstrates that this TCR was formed during an extremely quiet interval and did not appear to generate any enhancement in the auroral electrojets.

[29] Of a total of five events in the near-Earth group, three are associated with enhanced geomagnetic activity (as defined by $AL < -100$ nT). Of the 19 events in the further-downtail category, only 4 events can be related to active times. Figure 8 is a superposed epoch analysis of the *AL* index for 60 min before and after the observation of the flux ropes/TCRs at t_0. If a string of flux ropes are observed, t_0 is taken as the time of observation of the first one. As before,

Figure 7. (a) The *AL* index for a 4 h interval on 4 March 2009. (b–f) An NS flux rope observed by THEMIS C on the same day. (g) The *AL* index for a 4 h interval on 23 February 2009. (h–k) An SN TCR observed by THEMIS B on the same day. A vertical dashed line in each figure marks the center of the signature. The magnetic field data have the same format as that in Figure 2.

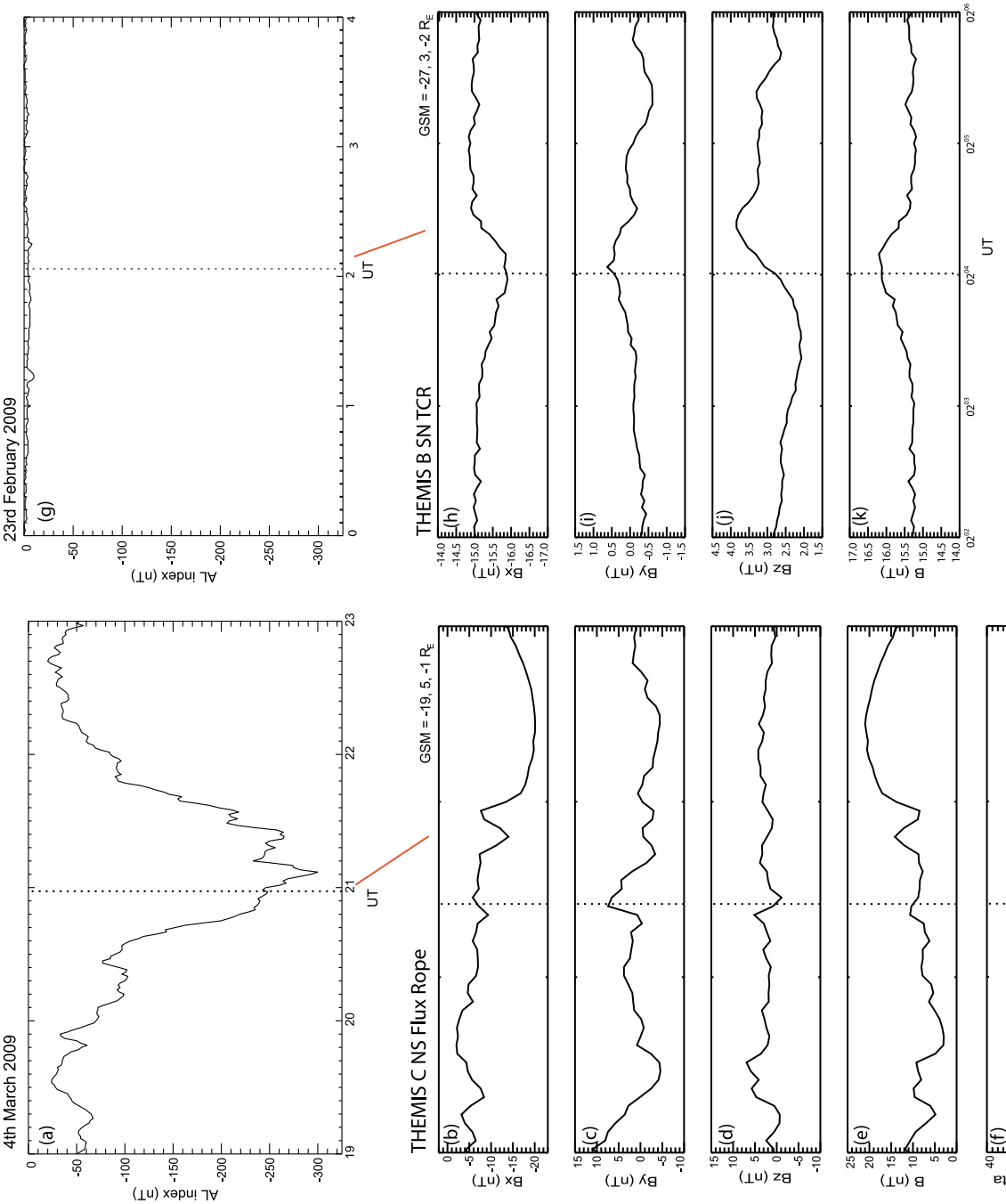
4th March 2009
23rd February 2009
THEMIS C NS Flux Rope
THEMIS B SN TCR
GSM = -19, 5, -1 R_E
GSM = -27, 3, -2 R_E
(a)
(b)
(c)
(d)
(e)
(f)
(g)
(h)
(i)
(j)
(k)
AL index (nT)
Bx (nT)
By (nT)
Bz (nT)
B (nT)
Plasma Beta
UT

Figure 7

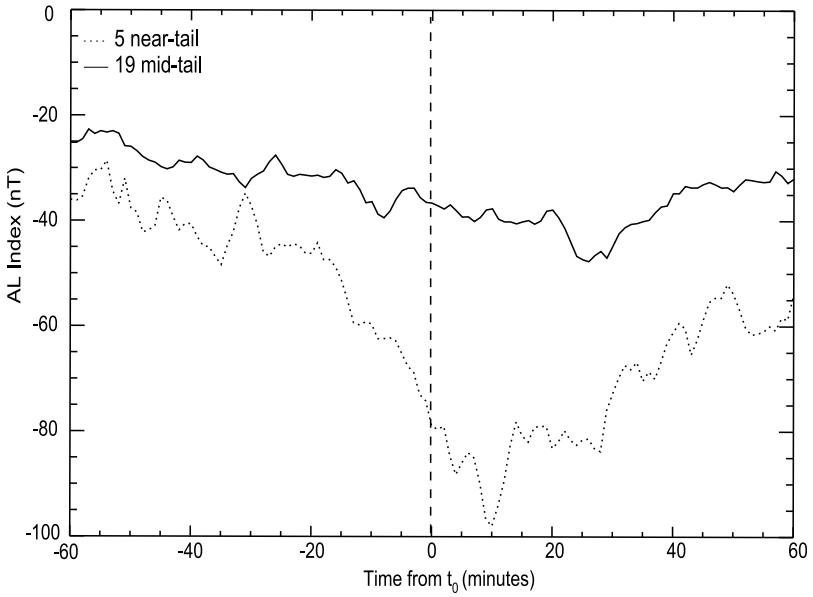

Figure 8. A superposed epoch analysis of the geomagnetic *AL* index from 60 min before until 60 min after the time at which the event was observed at THEMIS (t_0). The dashed line is for the 5 near-tail events, whereas the solid line is the 19 mid-tail events.

the dotted line is for the 5 events in which reconnection took place within −20 R_E, whereas the solid line is for the 19 events in which reconnection was initiated beyond −25 R_E. It is clear that more enhanced geomagnetic activity is observed when reconnection was initiated closer to the Earth. This result confirms that obtained in a statistical study by *Miyashita et al.* [2004], who used in situ Geotail measurements to show that for intense substorms the region of southward magnetic field associated with the plasmoid, as well as the first decrease in the total pressure are observed closer to the Earth. The t_0 is located just as the *AL* index is beginning to fall more steeply, indicating that the events tend to be observed during the expansion phase of a substorm. In contrast, reconnection taking place in the midtail region (in Figure 8, solid black trace) does not appear to have a significant impact on geomagnetic activity levels.

4.4. The Dawn-Dusk Location of the Reconnection Site

[30] The location and extent of the reconnection site in the dawn-dusk direction is a matter of some controversy, with the majority of (but not all) studies reporting asymmetric reconnection signatures in the east-west direction (Table 1). Figure 9a displays the number of events observed per hour of observation time (multiplied by a factor of 100) against the GSM Y* location of the observing spacecraft. The GSM Y locations have been corrected (Y*) for a solar aberration angle of 4°. A dashed vertical line is plotted through Y* = 0 to guide the eye. There is an obvious asymmetry in the observations, with 81% of all flux ropes/TCRs observed in the dusk sector. The mean location of the observing spacecraft was Y* = 5R_E. The solid black line is a Gaussian fit to the data; the peak of the Gaussian is at Y* = 7.0 R_E, and the full-width at half-maximum is 15.5 R_E.

[31] Figure 9b shows the location of the observing spacecraft in the GSM X-Y* plane, with red crosses for SN and blue crosses for NS events, and the dashed line marks

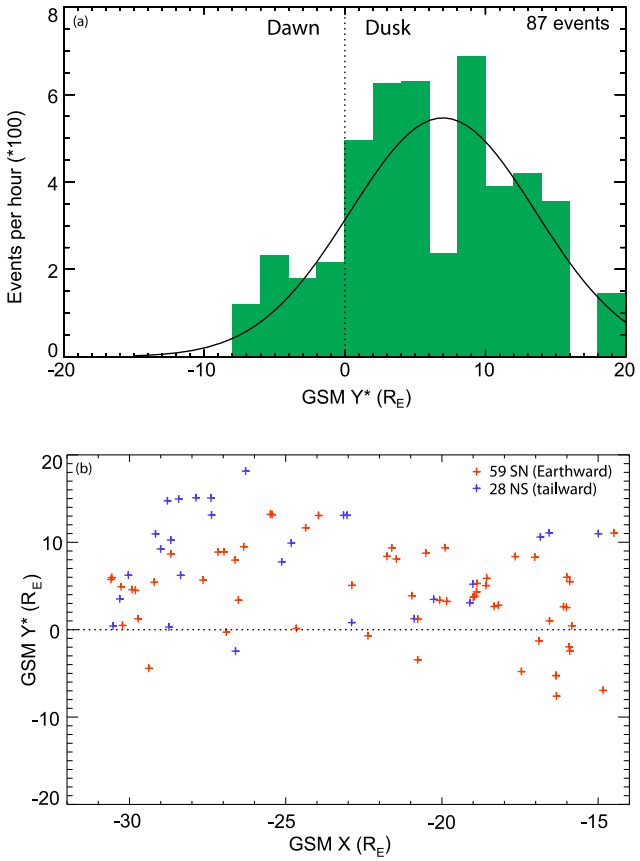

Figure 9. (a) The location of the spacecraft for all 87 FR/TCR observations in the GSM X-Y* plane (where Y* is GSM Y with a solar aberration angle correction). The dashed line marks Y* = 0. (b) The number of events per hour (*100) observed binned by the GSM Y* location of the observing spacecraft. The vertical dashed line is at Y* = 0, and the black curve is a Gaussian fit to the data.

$Y^* = 0$. The distribution is clearly broad and very skewed toward dusk beyond $X = -20$ R_E; however, it narrows between -18 and -20 R_E. Earthward of this location, the distribution broadens significantly, and the SN population appears to become more symmetric. Any asymmetry observed in the number of flux ropes identified is unlikely to be due to orbital or seasonal effects.

[32] We interpret the midtail asymmetry in both the Earthward and tailward moving FR/TCRs as being due to the reconnection site being preferentially located in the dusk as opposed to the dawn sector, although it is not clear why this should be the case. It is most likely associated with the tendency for ions to drift duskward within the plasma sheet. We postulate that the shift toward a more symmetric FR/TCR population within ~18 R_E is due to the diversion of the flow around the flux pileup region in the near-tail.

[33] No statistical in situ study of the length of flux ropes has yet been possible as this requires simultaneous multipoint measurements. In this study, we have assumed that the length of the earthward-moving and tailward-moving flux ropes are the same and do not change with time.

[34] The onset of substorms in the inner magnetosphere is also known to be asymmetric, with the auroral onset predominantly in the premidnight sector, later expanding azimuthally as the substorm develops [e.g., *Frey et al.*, 2004]. *Ieda et al.* [2001] used Geotail and Polar data to show the ionospheric footprint of plasmoids (observed between 21 and 29 R_E downtail) map closely to the location of auroral brightenings. *Fairfield et al.* [1999] also used Geotail and Polar data to show that high-velocity Earthward flow bursts observed by Geotail in the region 10–15 R_E downtail can be associated with auroral brightenings occurring very close to the footprint of the Geotail location. Contrary to these results, *Nakamura et al.* [2001] showed that Earthward flows in the region 10–30 R_E downtail map to regions 0.4 magnetic local time (MLT) east of auroral expansions. The rapidly changing magnetic field line configuration in the tail during reconnection renders accurate mapping of the THEMIS location to the ionosphere unreliable; however, an estimate using the average values of $(X_{GSM}, Y_{GSM}) = (-30R_E, 5R_E)$ gives a value of ~23 MLT. This is in agreement with the average auroral onset location of 23 MLT reported in a statistical study of IMAGE auroral data by *Frey et al.* [2004].

5. Conclusions

[35] We have identified 135 flux ropes/TCRs corresponding to 87 individual reconnection intervals using the outermost pair of THEMIS spacecraft. These observations were made during the second THEMIS tail season, which corresponded to a period of extremely low solar activity with slow solar wind velocity and low magnetic field strength. The ratio of Earthward to tailward moving events is used to determine that the average location of the near-Earth neutral line is GSM $X = -30$ R_E. This result is toward the tailward edge of previous estimates. We use superposed-epoch analysis to demonstrate that reconnection onset in the midtail ($X < -25$ R_E) is associated with slightly lower solar wind speed and less negative B_Z (i.e., weaker dayside driving) than for the near-tail ($X > -20$ R_E). We therefore suggest that the quiet solar wind conditions produced during the extended solar minimum resulted in the average reconnection site moving further downtail than during active times.

[36] The implication of the x-line location on the geomagnetic response has also been investigated. We have shown that reconnection closer to the Earth is related to enhanced geomagnetic activity (as measured by the *AL* index); however, when reconnection is initiated beyond -25 R_E, the geomagnetic response appears to be lower.

[37] The location and extent of the reconnection site in the dawn–dusk direction has been addressed by previous studies of reconnection signatures such as BBFs and flux ropes. Most of these have concluded that the reconnection site is more frequently located in the dusk sector (Table 1) although there is no consistent explanation for this bias. The distribution of our events in the east-west direction is significantly skewed toward dusk with a mean location of $Y^* = 5.0$ R_E. We find that the Earthward-moving events are skewed toward dusk beyond -18 R_E, but in contrast to previous studies, our distribution of Earthward events becomes more symmetric within -18 R_E. It is not clear what causes this; however, we postulate this effect could be due to the flux ropes slowing and being diverted around the flux pileup region. The average location of the reconnection site in the premidnight sector is in good agreement with auroral observations of substorm onset.

[38] **Acknowledgments.** We acknowledge NASA contract NAS5-02099, DLR contract 50 OC 0302, and C. W. Carlson and J. P. McFadden for use of ESA data.

[39] Masaki Fujimoto thanks the reviewers for their assistance in evaluating this paper.

References

Angelopoulos, V., C. F. Kennel, F. V. Coroniti, R. Pellat, M. G. Kivelson, R. J. Walker, C. T. Russell, W. Baumjohann, W. C. Feldman, and J. T. Gosling (1994), Statistical characteristics of bursty bulk flow events, *J. Geophys. Res.*, *99*, 21,257–21,280, 1994, doi:10.1029/94JA01263.

Auster, H. U., et al. (2008), The THEMIS Fluxgate Magnetometer, *Space Sci. Rev.*, *141*, 235–264, doi:10.1007/s11214-008-9365-9.

Baker, D. N., T. I. Pulkkinen, V. Angelopoulos, W. Baumjohann, and R. L. McPherron (1996), Neutral line model of substorms: Past results and present view, *J. Geophys. Res.*, *101*, 12,975–13,010, doi:10.1029/95JA03753.

Eastwood, J. P., D. G. Sibeck, J. A. Slavin, M. L. Goldstein, B. Lavraud, M. Sitnov, S. Imber, A. Balogh, E. A. Lucek, and I. Dandouras (2005), Observations of multiple X-line structure in the Earth's magnetotail current sheet: A Cluster case study, *Geophys. Res. Lett.*, *32*, L11105, doi:10.1029/2005GL022509.

Fairfield, D. H., et al. (1999), Earthward flow bursts in the inner magnetotail and their relation to auroral brightenings, AKR intensifications, geosynchronous particle injections and magnetic activity, *J. Geophys. Res.*, *104*, 355–370, doi:10.1029/98JA02661.

Frey, H. U., S. B. Mende, V. Angelopoulos, and E. F. Donovan (2004), Substorm onset observations by IMAGE-FUV, *J. Geophys. Res.*, *109*, A10304, doi:10.1029/2004JA010607.

Henderson, P. D., C. J. Owen, I. V. Alexeev, J. Slavin, A. N. Fazakerlay, E. Lucek, and H. Rème (2006), Cluster observations of flux rope structures in the near-tail, *Ann. Geophys.*, *24*, 651–666, doi:10.5194/angeo-24-651-2006.

Hesse, M., J. Birn, D. N. Baker, and J. A. Slavin (1996), MHD simulations of the transition of magnetic reconnection from closed to open field lines, *J. Geophys. Res.*, *101*, 10,805–10,816.

Hill, T. W., et al. (2008), Plasmoids in Saturn's magnetotail, *J. Geophys. Res.*, *113*, A01214, doi:10.1029/2007JA012626.

Hones, E. W., Jr. (1977), Substorm processes in the magnetotail: Comments on "On hot tenuous plasma, fireballs, and boundary layers in the Earth's magnetotail" by L. A. Frank, K. L. Ackerson, and R. P. Lepping, *J. Geophys. Res.*, *82*, 5633–5640, doi:10.1029/JA082i035p05633.

Hones, E. W., Jr., and K. Schindler (1979), Magnetotail Plasma Flow During Substorms: A Survey with Imp 6 and Imp 8 Satellites, *J. Geophys. Res.*, *84*, 7155–7169, doi:10.1029/JA084iA12p07155.

Hones, E. W., Jr., J. Birn, D. N. Baker, S. J. Bame, W. C. Feldman, D. J. McComas, R. D. Zwickl, J. A. Slavin, E. J. Smith, and B. T. Tsurutani (1984), Detailed examination of a plasmoid in the distant magnetotail with ISEE 3, *Geophys. Res. Lett.*, *11*, 1046–1049, doi:10.1029/GL011i010p01046.

Ieda, A., S. Machida, T. Mukai, Y. Saito, T. Yamamoto, A. Nishida, T. Terasawa, and S. Kokubun (1998), Statistical analysis of plasmoid evolution with Geotail observations, *J. Geophys. Res.*, *103*, 4453–4465, doi:10.1029/97JA03240.

Ieda, A., D. H. Fairfield, T. Mukai, Y. Saito, S. Kokubun, K. Liou, C.-I. Meng, G. K. Parks, and M. J. Brittnacher (2001), Plasmoid ejection and auroral brightenings, *J. Geophys. Res.*, *106*, 3845–3857, doi:10.1029/1999JA000451.

Jackman, C. M., C. T. Russell, D. J. Southwood, C. S. Arridge, N. Achilleos, and M. K. Dougherty (2007), Strong rapid dipolarizations in Saturn's magnetotail: In situ evidence of reconnection, *Geophys. Res. Lett.*, *34*, L11203, doi:10.1029/2007GL029764.

Kan, J. R., and L. C. Lee (1979), Energy coupling function and solar wind magnetosphere dynamo, *Geophys. Res. Lett.*, *6*, 577–580, doi:10.1029/GL006i007p00577.

Kawano, H., T. Yamamoto, S. Kokubun, K. Tsuruda, A. T. Y. Lui, D. J. Williams, K. Yumoto, H. Hayakawa, M. Nakamura, and T. Okada (1994), A flux rope followed by recurring encounters with traveling compression regions: GEOTAIL observations, *Geophys. Res. Lett.*, *21*, 2891–2894, doi:10.1029/94GL02101.

Kronberg, E. A., K.-H. Glassmeier, J. Woch, N. Krupp, A. Lagg, and M. K. Dougherty (2007), A possible intrinsic mechanism for the quasi-periodic dynamics of the Jovian magnetosphere, *J. Geophys. Res.*, *112*, A05203, doi:10.1029/2006JA011994.

McFadden, J. P., C. W. Carlson, D. Larson, M. Ludlam, R. Abiad, B. Elliott, P. Turin, M. Marckwordt, and V. Angelopoulos (2008), The THEMIS ESA plasma instrument and in-flight calibration, *Space Sci. Rev.*, *141*, 277–302, doi:10.1007/s11214-008-9440-2.

Miyashita, Y., Y. Kamide, S. Machida, K. Liou, T. Mukai, Y. Saito, A. Ieda, C.-I. Meng, and G. K. Parks (2004), Difference in magnetotail variations between intense and weak substorms, *J. Geophys. Res.*, *109*, A11205, doi:10.1029/2004JA010588.

Moldwin, M. B., and W. J. Hughes (1992), On the formation and evolution of plasmoids: A survey of ISEE 3 Geotail data, *J. Geophys. Res.*, *97*, 19,259–19,282, doi:10.1029/92JA01598.

Nagai, T. (2006), Location of magnetic reconnection in the magnetotail, *Space Sci. Rev.*, *122*, 39–54, doi:10.1007/s11214-006-6216-4.

Nagai, T., and S. Machida (1998), Magnetic reconnection in the near-Earth magnetotail, in *New Perspectives on the Earth's Magnetotail*, *Geophys. Monogr. Ser.*, vol. 105, edited by A. Nishida, D. N. Baker, and S. W. H. Cowley, pp. 211–224, AGU, Washington, D. C.

Nagai, T., M. Fujimoto, Y. Saito, S. Machida, T. Terasawa, R. Nakamura, T. Yamamoto, T. Mukai, A. Nishida, and S. Kokubun (1998), Structure and dynamics of magnetic reconnection for substorm onsets with Geotail observations, *J. Geophys. Res.*, *103*, 4419–4440, doi:10.1029/97JA02190.

Nagai, T., M. Fujimoto, R. Nakamura, W. Baumjohann, A. Ieda, I. Shinohara, S. Machida, Y. Saito, and T. Mukai (2005), Solar wind control of the radial distance of the magnetic reconnection site in the magnetotail, *J. Geophys. Res.*, *110*, A09208, doi:10.1029/2005JA011207.

Nakamura, R., G. Paschmann, W. Baumjohann, and N. Sckopke (1991), Ion distributions and flows near the neutral sheet, *J. Geophys. Res.*, *96*, 5631–5649, doi:10.1029/90JA02495.

Nakamura, R., W. Baumjohann, R. Schödel, M. Brittnacher, V. A. Sergeev, M. Kubyshkina, T. Mukai, and K. Liou (2001), Earthward flow bursts, auroral streamers, and small expansions, *J. Geophys. Res.*, *106*, 10,791–10,802, doi:10.1029/2000JA000306.

Nishida, A., H. Hayakawa, and E. W. Hones Jr. (1981), Observed signatures of reconnection in the magnetotail, *J. Geophys. Res.*, *86*, 1422–1436, doi:10.1029/JA086iA03p01422.

Ohtani, S., K. Takahashi, L. J. Zanetti, T. A. Potemra, R. W. McEntire, and T. Iijima (1992), Initial signatures of magnetic field and energetic particle fluxes at tail reconfiguration: Explosive growth phase, *J. Geophys. Res.*, *97*, 19,311–19,324.

Raj, A., T. Phan, R. P. Lin, and V. Angelopoulos (2002), Wind survey of high-speed bulk flows and field-aligned beams in the near-Earth plasma sheet, *J. Geophys. Res.*, *107*(A12), 1419, doi:10.1029/2001JA007547.

Runov, A., V. Angelopoulos, M. I. Sitnov, V. A. Sergeev, J. Bonnell, J. P. McFadden, D. Larson, K.-H. Glassmeier, and U. Auster (2009), THEMIS observations of an earthward propagating dipolarization front, *Geophys. Res. Lett.*, *36*, L14106, doi:10.1029/2009GL038980.

Saito, M. H., L.-N. Hau, C.-C. Hung, Y.-T. Lai, and Y.-C. Chou (2010), Spatial profile of magnetic field in the near-Earth plasma sheet prior to dipolarization by THEMIS: Feature of minimum B, *Geophys. Res. Lett.*, *37*, L08106, doi:10.1029/2010GL042813.

Schindler, K. (1974), A theory of the substorm mechanism, *J. Geophys. Res.*, *79*, 2803–2810, doi:10.1029/JA079i019p02803.

Sergeev, V., V. Angelopoulos, S. Apatenkov, J. Bonnell, R. Ergun, R. Nakamura, J. McFadden, D. Larson, and A. Runov (2009), Kinetic structure of the sharp injection/dipolarization front in the flow-braking region, *Geophys. Res. Lett.*, *36*, L21105, doi:10.1029/2009GL040658.

Shay, M. A., J. F. Drake, M. Swisdak, and W. Dorland (2003), Inherently three dimensional magnetic reconnection: A mechanism for bursty bulk flows?, *Geophys. Res. Lett.*, *30*(6), 1345, doi:10.1029/2002GL016267.

Sibeck, D. G., and V. Angelopoulos (2008), THEMIS science objectives and mission phases, *Space Sci. Rev.*, *141*, 35–59, doi:10.1007/s11214-008-9393-5.

Sibeck, D. G., G. L. Siscoe, J. A. Slavin, E. J. Smith, S. J. Bame, and F. L. Scarf (1984), Magnetotail flux ropes, *Geophys. Res. Lett.*, *11*, 1090–1093, doi:10.1029/GL011i010p01090.

Sitnov, M. I., M. Swisdak, and A. V. Divin (2009), Dipolarization fronts as a signature of transient reconnection in the magnetotail, *J. Geophys. Res.*, *114*, A04202, doi:10.1029/2008JA013980.

Slavin, J. A., E. J. Smith, B. T. Tsurutani, D. G. Sibeck, H. J. Singer, D. N. Baker, J. T. Gosling, E. W. Hones, and F. L. Scarfs (1984), Substorm associated traveling compression regions in the distant tail: ISEE-3 Geotail observations, *Geophys. Res. Lett.*, *11*, 657–660, doi:10.1029/GL011i007p00657.

Slavin, J. A., M. F. Smith, E. L. Mazur, D. N. Baker, E. W. Hones Jr., T. Iyemori, and E. W. Greenstadt (1993), ISEE 3 observations of traveling compression regions in the Earth's magnetotail, *J. Geophys. Res.*, *98*, 15,425–15,446, doi:10.1029/93JA01467.

Slavin, J. A., et al. (1998), ISTP observations of plasmoid ejection: IMP 8 and Geotail, *J. Geophys. Res.*, *103*, 119–133.

Slavin, J. A., R. P. Lepping, J. Gjerloev, D. H. Fairfield, M. Hesse, C. J. Owen, M. B. Moldwin, T. Nagai, A. Ieda, and T. Mukai (2003), Geotail observations of magnetic flux ropes in the plasma sheet, *J. Geophys. Res.*, *108*(A1), 1015, doi:10.1029/2002JA009557.

Slavin, J. A., E. I. Tanskanen, M. Hesse, C. J. Owen, M. W. Dunlop, S. Imber, E. A. Lucek, A. Balogh, and K.-H. Glassmeier (2005), Cluster observations of traveling compression regions in the near-tail, *J. Geophys. Res.*, *110*, A06207, doi:10.1029/2004JA010878.

Slavin, J. A., et al. (2009), MESSENGER observations of magnetic reconnection in Mercury's magnetosphere, *Science*, *324*(5927), 606–610, doi:10.1126/science.1172011.

Taguchi, S., J. A. Slavin, R. P. Lepping, and M. Nosé (1996), Travelling compression region observed in the mid-tail lobes near substorm expansion phase onset, in *Proceedings of the Third International Conference on Substorms*, edited by E. J. Rolfe and B. Kaldeich, p. 603, Eur. Space Agency, Paris.

Taguchi, S., J. A. Slavin, and R. P. Lepping (1998), Traveling compression regions in the midtail: Fifteen years of IMP 8 observations, *J. Geophys. Res.*, *103*, 17,641–17,650, doi:10.1029/98JA01206.

Vogt, M. F., M. G. Kivelson, K. K. Khurana, S. P. Joy, and R. J. Walker (2010), Reconnection and flows in the Jovian magnetotail as inferred from magnetometer observations, *J. Geophys. Res.*, *115*, A06219, doi:10.1029/2009JA015098.

V. Angelopoulos, Institute of Geophysics and Planetary Physics, University of California, Los Angeles, CA 90095, USA.

H. U. Auster, Institut für Geophysik und Extraterrestrische Physik, Technische Universität Braunschweig, Braunschweig D-38106, Germany.

S. M. Imber and J. A. Slavin, NASA Goddard Space Flight Center, Code 670.0, Bldg. 21, Greenbelt Rd., Greenbelt, MD 20771, USA. (suzanne.imber@nasa.gov)